Broadband Permittivity of Liquids Extracted from Transmission Line Measurements of Microfluidic Channels*

Jordi Mateu, Nathan Orloff, Matt Rinehart, James C. Booth

National Institute of Standards and Technology, Boulder, CO, USA

Abstract — **We present a semi-analytical procedure to extract the permittivity of fluids from measurements in our microfluidic-microelectronic platform. This platform consists of broadband coplanar waveguide transmission lines with integrated microfluidic channels for characterizing the dielectric properties of submicroliter fluid samples. On-wafer calibration techniques are used to obtain the S-parameters of the composite structure (transmission line and microfluid channel) up to 40 GHz. Using microwave network analysis theory, we isolated the response of the microfluidic channel. We modeled the microfluidic channel as a distributed transmission line segment and as a single RLCG elemental segment. Both approaches analytically yield the circuit capacitance C_F and conductance G_F per unit length of the segment incorporating the microfluidic channel. A finite element electromagnetic simulator is then used to obtain the permittivity of the fluid as a continuous function of frequency. We applied this technique to extract the permittivity of submicroliter liquid volumes. Here we present results on polystyrene latex beads suspended in an aqueous solution over the frequency range from 100 MHz to 40 GHz.**

Index Terms — **coplanar wave-guides, microfluidic measurements, permittivity measurements.**

I. Introduction

Characterization of liquid and biological samples is important in research and increasingly in surveillance and clinical applications. Electromagnetic characterization is emerging as an alternative to typical chemical and photonic detection schemes. One promising electromagnetic detection technique is dielectric spectroscopy, which characterizes the permittivity of the fluid as a continuous function of frequency. Permittivity measurements can yield important information on composition of liquids and cell suspensions, such as cell structure, orientation of molecular dipoles, and surface conductance [1], [2]. Electrical characteristics of liquids and biological samples, which can be related to their chemical composition, demand efficient measurement techniques that can be applied over a broad frequency range.

Our technique is based on a measurement platform that integrates microfluidics and microelectronics in order to characterize the electromagnetic properties of submicroliter fluid volumes up to 40 GHz [3]. Fig.1 shows, as an example, a measurement platform that contains multiple patterned coplanar waveguide (CPW) transmission lines integrated with a microfluidic channel formed in a slab of the elastomer polydimethylsiloxane (PMDS). Details on the fabrication of the microfluidic test structures can be found in [3]. The measurements presented in this paper have been performed with the platform of Fig. 1. Calibration structures are also patterned in the same chip (see lower part of Fig.1). The multiple patterned devices and calibration structures were accessed by a microwave probe station for a rapid and accurate broadband characterization of the fluid properties. Using this technique, we previously presented results for water and methanol over a broad frequency range, from 100 Hz to 40 GHz [3].

The broadband measurements of an entire transmission line were then used to isolate the response of the segment containing the microfluidic channel. This analysis yields the conductance G_F and capacitance C_F per unit length of the transmission line segment loaded by the fluid within the microfluidic channel. This paper details the semi-analytical procedure to extract C_F and G_F from S-parameter measurements of broadband CPW transmission lines. Fast and accurate extraction of the parameters of the microchannel region is essential for a full exploitation of our microelectronic-microfluidic technique. The conductance and capacitance are then reduced to the dielectric properties of the fluid (permittivity) by use of a finite element electromagnetic simulator.

We used this procedure to extract the permittivity of an aqueous solution with suspended 3 μm polystyrene latex beads over the frequency range from 100 MHz to 40 GHz. Differences between measured and the estimated results from the extracted permittivity are less than 5 % over the entire frequency range.

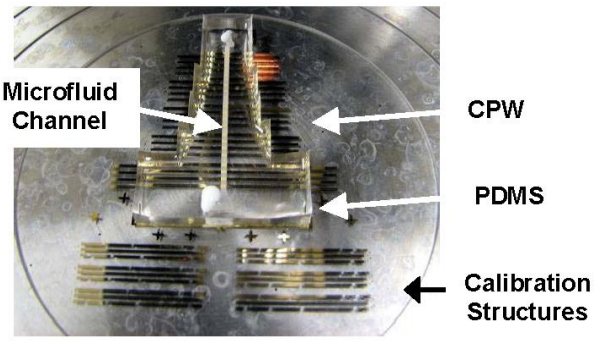

Fig. 1. Microfluidic-microelectronic measurement platform.

* Contribution of the U.S. government; not subject to U.S. copyright.

II. Test Structures and Measurements

The measurement platform of Fig. 1 contains three sets of CPW transmission lines fabricated from 0.4 μm thick Ti/Au conductors deposited on a 75 mm diameter quartz substrate. The center conductor width of each set of lines is 50 μm, and the gaps between the center conductors and ground planes are 10 μm, 20 μm and 50 μm. The PDMS slab is centered on top of the lines with a centered straight microfluidic channel connecting two larger fluid reservoirs (see Fig. 1). Figures 2a and 2b show respectively a top view and cross section of a transmission line with the microfluidic channel for the measurement platform shown in Fig. 1. The width (l_F) and depth (h) of the microchannel are 0.985 mm and 28 μm, respectively, and are the same for all the transmission lines on our measurement platform. The CPW transmission lines of each set have a different total length l_T ($=2l_A+2l_P+l_F$), where l_A is the length of the substrate/air region, and l_P is the length of the substrate/PDMS region. The total width of the PDMS region is l_{PDMS}, which includes the microchannel ($l_{PDMS}=2l_P+l_F$). The lengths of the transmission lines and their corresponding PDMS segments are detailed in Table I.

On-wafer multiline thru-reflect-line (TRL) calibrations were performed using the calibration structures embedded on the same wafer, and were used to obtain accurate S-parameter measurement of the test CPW/microchannel structures from 100 MHz to 40 GHz.

III. Analytical Formulation

From the measurements above, we obtained S-parameters of the test structures calibrated to 50 Ω with the reference planes translated to the location of the microwave wafer probes. We analyzed these measurements to isolate the response of the fluid segment by using network analysis theory [4]. To do this, we start modeling our CPW/microchannel structures (Fig. 2a) as a concatenation of different transmission line segments.

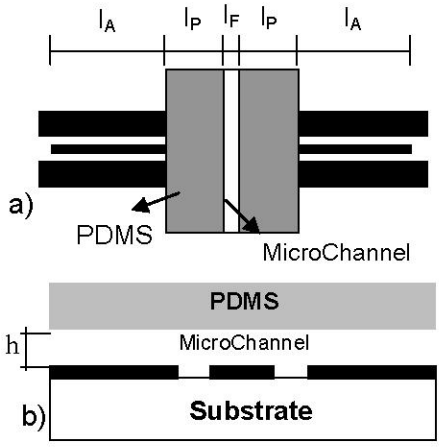

Fig. 2. Schematic of our microfluidic-microelectronic platform. (a) Top view of a CPW transmission line with the microchannel integrated on top. (b) Cross-section of microchannel and CPW transmission line. The length of the CPW l_T is equal to $2l_A+2l_P+l_F$, the total width of the PDMS l_{PDMS} is $2l_P+l_F$. Table I details the dimensions of the lines.

TABLE I
Lengths of Transmission Lines and PDMS Sections

l_T (mm)	20.0	22.135	23.2	26.565
l_{PDMS} (mm)	9.852	11.956	13.005	16.32

Figure 3 outlines this equivalent circuit model, where Z_A, γ_A, Z_P, γ_P, and Z_F and γ_F are respectively the characteristic impedances and propagation constants of the transmission line segments with bare lines (substrate/air region), lines with solid PDMS on top (substrate/PDMS region), and the microfluidic channel region (substrate/channel region). From this equivalent circuit we can write the ABCD matrix of the whole structure M_S as

$$M_S = M_A \cdot M_P \cdot M_{FLUID} \cdot M_P \cdot M_A , \quad (1)$$

where M_A, M_P and M_{FLUID} are respectively the ABCD matrices of the bare line segment of length l_A, the line segment with PDMS on top, of length l_P, and the microchannel segment of length l_F.

Using (1), we isolate the response of the microfluid channel as

$$M_{FLUID} = M_P^{-1} \cdot M_A^{-1} \cdot M_S \cdot M_A^{-1} \cdot M_P^{-1} . \quad (2)$$

Note that we need to know the response of the entire structure, M_S, the response of the bare lines, M_A and the response of the line segments with PDMS on top, M_P. Accurate knowledge of these responses, M_S, M_A and M_P, will define the accuracy of the extracted response of the microfluidic section.

As mentioned above, on-wafer calibration techniques of the entire measurement structure ensure sufficient accuracy of M_S. Note that M_S is obtained by converting the measured S-parameters to the corresponding ABCD matrix, with $Z_0 = 50\ \Omega$ [4].

The response of the bare line segments M_A have been extracted from calibrated measurements on bare CPW transmission lines before affixing the PDMS slab on the test wafer. With multiline TRL calibrations we obtained the propagation constant of the bare lines. Measurements of lumped resistor standards (also embedded in the platform) allowed us to obtain the distributed transmission line capacitances [5][6]. From the propagation constants and the distributed capacitance, we obtained the characteristic impedances of the lines [7]. Combining the characteristic impedances and the propagation constants we extracted the RLCG distributed parameters of the lines, which are referred to as R_A, L_A, C_A and G_A, for the bare lines. To create M_A we do not need to extract the distributed parameters. However, these parameters will be also used to model the PDMS and microfluid segments. Note that in a TEM propagation mode

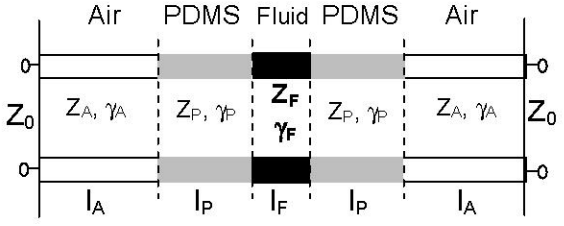

Fig. 3. Distributed transmission line equivalent-circuit model of one test structure of our microfluidic-microelectronic platform.

the distributed resistance R_A and inductance L_A are entirely due to the metallic conductors and are the same throughout the entire transmission line. To reduce uncertainties in R_A and L_A due to measurement error, we refined these values with electromagnetic simulations calculated from the measured DC resistivity of the transmission lines [8] and the transmission line dimensions. On the other hand, to obtain the distributed capacitance C_P and conductance G_P of the PDMS segment we performed measurements on structures with a solid PDMS slab, without the microchannel [3]. Then, directly from the distributed parameters of bare transmission lines L_A, R_A, C_A and G_A and the parameters of the PMDS segments L_A, R_A, C_P and G_P, we constructed the ABCD matrices by modeling the bare transmission line segments M_A and the transmission lines with PMDS slab M_P. Then using (2), with the measured response of the structure M_S and the modeled transmission line segments M_A and M_P, we determined the response of the microchannel transmission line segment M_{FLUID}.

Since we are primarily interested in the fluid properties, we wish to extract the distributed capacitance C_F and conductance G_F of the microchannel transmission line segment. These distributed parameters (L_A, R_A, C_F and G_F) give rise to an estimated microchannel response M_{FLUID_E} that can be used to calculate an estimated response of the whole structure M_{S_E}, using (1). C_F and G_F must be chosen in order to minimize the difference between the measured S-parameters S and the S-parameters S' resulting from M_{FLUID_E}, i.e., as the minimum of ($\Sigma|S_{ij} - S'_{ij}|$), where the sum runs over all four elements of the S-parameter matrix.

We used two different approaches to extract C_F and G_F, a *distributed* approach and a *singl- cell lumped* approach.

A. Distributed Approach

The distributed approach consists of modeling the microchannel as a transmission line segment of length l_F, as shown in the equivalent circuit of Fig. 4. Therefore the response extracted from the measurements M_{FLUID} should be of the form

$$\begin{bmatrix} \cosh(\gamma_F l_F) & Z_F \sinh(\gamma_F l_F) \\ \frac{1}{Z_F}\sinh(\gamma_F l_F) & \cosh(\gamma_F l_F) \end{bmatrix}, \quad (3)$$

where the characteristic impedance Z_F and the propagation constant γ_F are related to the distributed parameters R_A, L_A, C_F and G_F. Since R_A and L_A are known, C_F and G_F can be analytically extracted from any of the matrix components (i.e., A, B, C, or D), which results in an overdetermined problem. We use the analytically extracted C_F and G_F as an initial guess for the iterative procedure, which consists of a least-squares function, to obtain the values of C_F and G_F that minimize $\Sigma|S_{ij} - S'_{ij}|$.

The distributed approach is fast and efficient at higher frequencies, where the initial C_F and G_F are close to the values that minimize the error. However, at lower frequencies this distributed approach is very sensitive to measurement uncertainties and the iterative procedure becomes inefficient or unstable. A second approach is proposed below to obtain the initial guesses and improve the efficiency of the iterative procedure at lower frequencies.

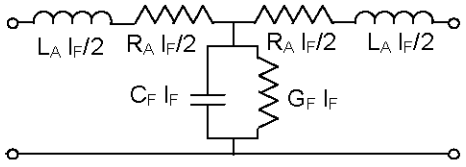

Fig. 4. Lumped equivalent circuit model of the microchannel transmission line segment.

B. Single Cell Lumped Approach

This approach models the microchannel as a single RLCG cell like the one shown in Fig. 4. The C term of the ABCD matrix of the equivalent circuit of Fig. 4 is [4]:

$$(G_F + j\omega C_F) l_F, \quad (4)$$

where ω is the angular frequency.

Equating (4) with the extracted response of the microchannel M_{FLUID} from (2), we obtain the C_F and G_F. These values are then used as initial guesses in our iterative procedure. In contrast with the distributed approach above, these initial guess values diverge at higher frequencies. Simple examination of the resulting error is used to determine the frequency range for which each approach is best for determining the initial guess for an efficient iterative procedure. Note that this procedure also would work in the case of non-symmetric structures; that is, for structures where the channel or the PMDS are not centered into the transmission line. In those cases, a previous step to obtain an estimate of the misalignment is required [3].

We have previously applied this measurement technique to different liquids in the measurement platform of Fig. 1 [3]. The next section illustrates the application of this analysis procedure to polystyrene latex beads in an aqueous suspension as the experimental fluid-under-test.

IV. Samples and Results

We applied the above procedure to extract the permittivity of an aqueous suspension containing 10 % by weight polystyrene latex beads of 3.0 μm mean particle size. Figure 5 shows the error $\Sigma|S_{ij} - S'_{ij}|$ at each frequency point when S' is obtained using: (i) the initial guess C_F and G_F from the single cell lumped approach (dotted line), (ii) the initial guess C_F and G_F from the distributed approach (thin-solid line) and (iii) the C_F and G_F resulting after the iteration procedure (thick-solid line). These results corroborate our assumption that the initial guess obtained from the distributed approach is close to the optimized values at higher frequencies but strongly deviates at lower frequencies (< 3 GHz). In contrast, the single cell lumped approach gives initial guess values that are close to the

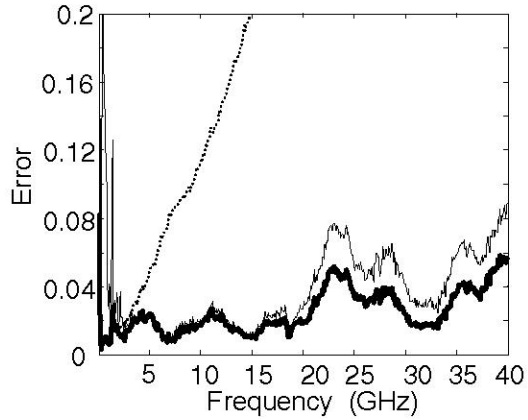

Fig. 5. Error as a function of frequency. Dotted, thin-solid and thick-solid lines respectively represent the error using the values obtained from the lumped approach, distributed approach and the values after the iterative procedure.

optimized values at lower frequencies but exhibit a large deviation at higher frequencies. In this case, we used the initial guess from the single cell lumped approach for frequencies up to 3 GHz and used the initial guess from the distributed approach at frequencies above 3 GHz.

Figure 6 shows the values of C_F and G_F resulting from the iterative procedure for the three sets of CPW structures. Solid lines, dashed lines and dotted lines indicate respectively C_F and G_F for the sets with 10 μm, 20 μm and 50 μm gap. Since the C_F and G_F terms depend on the specific geometry of the test structure, we reduced them to the fluid permittivity ε_r. Fig. 7 shows the real and imaginary part of the fluid permittivity from 100 MHz to 40 GHz, extracted from three different geometries. Solid, dashed and dotted lines correspond to the permittivity obtained from the set of CPW lines with 10 μm, 20 μm and 50 μm, respectively, showing consistency within +/- 5 %. Note that the biggest deviation occurs for the 50 μm gap structure, since this geometry is more sensitive to measurement errors due to the smaller values for the capacitance per unit length.

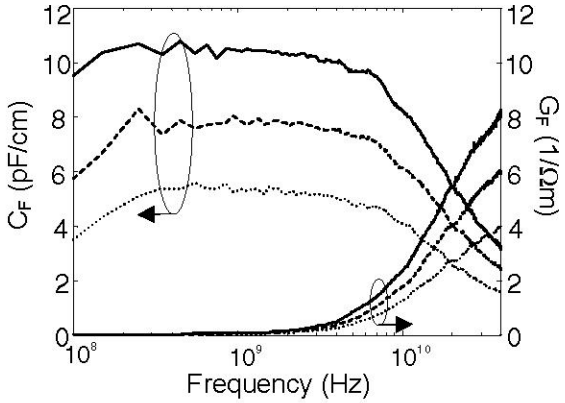

Fig. 6. Measured C_F and G_F for the three sets of measured CPW transmission lines. Solid, dashed and dotted lines correspond respectively to 10 μm, 20 μm and 50 μm gap.

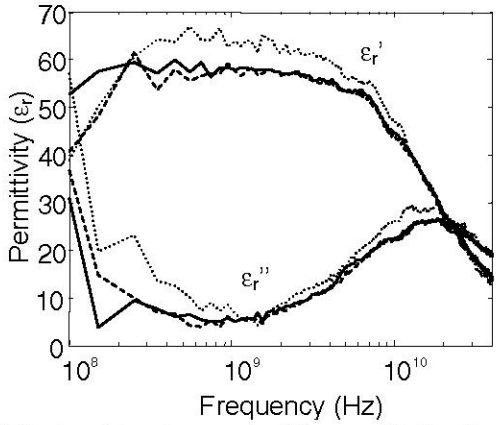

Fig. 7. Real and imaginary part of the permittivity of an aqueous solution containing 10% of polystyrene latex bead suspended particles. Solid, dashed and dotted lines corresponds respectively to measurements from lines with 10 μm, 20 μm and 50 μm gap.

V. Conclusions

We presented a semi-analytical procedure to extract the dielectric properties of liquid using our microfluidic/ microelectronic approach. The procedure allows us to rapidly and efficiently extract the dielectric properties from microwave measurements up to 40 GHz, although the procedure is not restricted to this frequency range. We successfully applied this procedure to microfluid structures with different transmission line geometries, and demonstrated the extraction of consistent values for the permittivity of an aqueous suspension of polystyrene latex beads.

References

[1] G. C. Facer, D. A. Notterman, L. L. Sohn, "Dielectric spectroscopy for bioanalysis: From 40 Hz to 26.5 GHz in microfabricated waveguide," *Appl. Lett.* 78, pp. 996-998 (2001).

[2] J. Baker-Jarvis "Measuring the permittivity and permeability of lossy materials: solid, liquids, metals, bulding materials, and negative-index materials" NIST Tech. Note 1536, 2005.

[3] J. C. Booth, J. Mateu, M. Janezic, "Broadband Permittivity Measurements of Liquid and Biological Samples using Microfluidic Channels," *2006 IEEE MTT-S Int. Microwave Symp. Dig.*, pp. 1750-1753, June 2006.

[4] D. M. Pozar, *Microwave Engineering*, New York: J. Wiley & Sons, Inc. 1998

[5] R. B. Marks, "A multiline method for Network analyzer calibration" *IEEE Trans. On Microwave Theory and Tech.* vol. 39, no. 7, pp. 1205-1215, 1991.

[6] D. F. Williams, R. B. Marks, "Transmission line capacitance measurements", *IEEE Microwave and Guided wave lett.*, vol., 1, no. 9, Sept. 1991.

[7] R. B. Marks, D. F. Williams, "Characteristic Impedance determination using propagation constant measurements". *IEEE Microwave and Guided wave Lett.*, vol., 1, no. 6, Sept. 1991.

[8] J. Mateu, J.C. Booth, S. A. Schima, "Characterization of the nonlinear response in ferroelectric thin-film transmission lines," submitted to *IEEE Trans. on Microwave Theory and Tech.*